

Detection of anthropogenic influence on the evolution of record-breaking temperatures over Europe

Margot Bador¹ · Laurent Terray¹ · Julien Boé¹

Received: 12 June 2014 / Accepted: 22 June 2015
© Springer-Verlag Berlin Heidelberg 2015

Abstract Changes in temperature extreme events are expected as a result of anthropogenic climate change, but uncertainties exist in when and how these changes will be manifest regionally. This is especially the case over Europe due to different methodologies and definitions of temperature extreme events. An alternative approach is to examine changes in record-breaking temperatures. Datasets of observed temperature combined with ensembles of climate model simulations are used to assess the possible causes and significance of record-breaking temperature changes over the late twentieth and twenty-first centuries. A simple detection methodology is first applied to evaluate the extent to which the effect of anthropogenic forcing can be detected in present-day observed and simulated changes in record-breaking temperature. We then study the projected evolution of record-breaking daily minimum and maximum temperatures over the twenty-first century in Europe with a climate model. The same detection approach is used to identify the time of emergence of the anthropogenic signal relative to a model-derived estimate of internal variability. From the 1980s onwards, a change in the evolution of cold and warm records is observed and simulated, but it still remains in the range of internal variability until the end of the twentieth century. Minimum and maximum

record-breaking temperatures tend to occur (respectively) less and more often than during the 1960s and 1970s taken as representative of a stationary climate. Model simulations with natural forcing only fail to reproduce the observed changes after the 1980s while the latter are compatible with simulations constrained by anthropogenic forcings. The deviation from the characteristic behavior of a stationary climate record-wise initiated in the 1980s is projected to accentuate during the twenty-first century. Annual changes become inconsistent with the model-derived internal variability between the 2020s and 2030s. Over the last three decades of the twenty-first century and under the RCP8.5 scenario, warm records occur on average five times more often than initially. Conversely, breaking new cold record become extremely difficult. The Mediterranean region is particularly affected in summer, whereas central and north-eastern Europe is more impacted in winter.

Keywords Temperature record-breaking statistics · Detection · Internal variability · Extreme events · Climate change

1 Introduction

Anthropogenic greenhouse gas emissions have already been proven to influence the Earth climate (IPCC AR4 and AR5 2007, 2013). How extreme climate events will be impacted is among the greatest challenges of climate science. The occurrence of extreme temperature events has increased steadily over the last few decades (Hansen et al. 2012), and links have been found between their increase and human influence (Coumou and Rahmstorf 2012). The Intergovernmental Panel on Climate Change (IPCC) reveals, in his special report on extreme events (SREX

✉ Margot Bador
bador@cerfacs.fr
Laurent Terray
terray@cerfacs.fr
Julien Boé
boe@cerfacs.fr

¹ Climate Modelling and Global Change Team, URA1875
CNRS/CERFACS, 42 Avenue G. Coriolis, 31057 Toulouse,
France

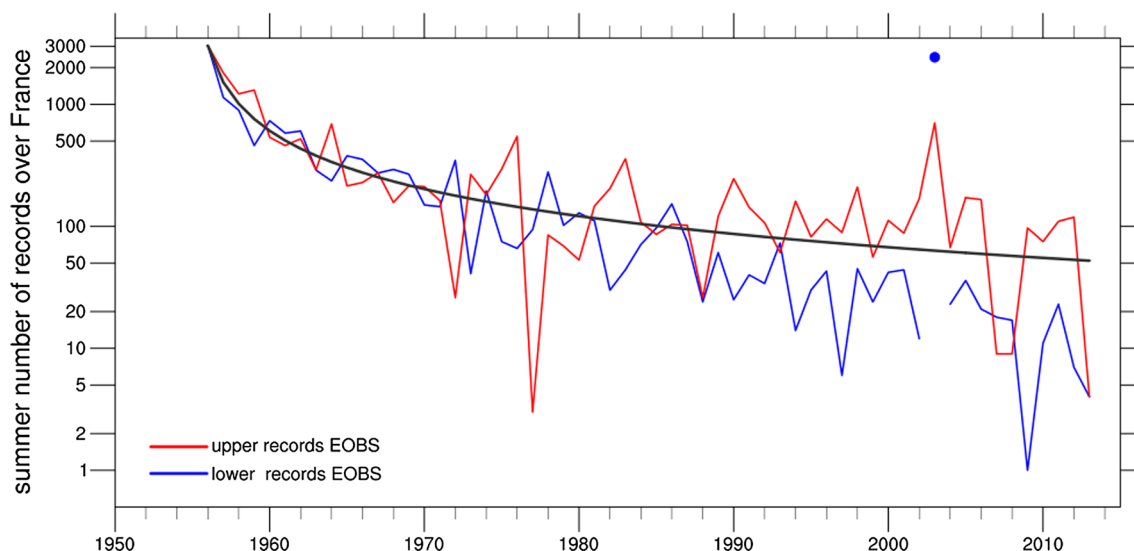


Fig. 1 Evolution of the summer number of upper (*red*) and lower (*blue*) records summed over France in the E-OBS observations, from 1956 to 2013. The record evolution expected in a stationary climate is represented by the *dark grey line*. The *dot* notifies a year of zero-

record occurrences over the entire French domain and illustrates here the impacts of the 2003 European heat wave. Caution needs to be taken with the logarithmic scale of the Y-axis

report, IPCC 2012), a *likely* decrease in the frequency of observed daily cold temperature extremes, along with an increase in the frequency of warm temperature extremes over Europe. This contrasted behavior is assessed to be *virtually certain* to continue in the twenty-first century.

The last decade is described as the warmest since 1500 (Barriopedro et al. 2011) and it is very likely that the length, frequency and intensity of heat waves will increase during the twenty-first century over most land areas (SREX report, IPCC 2012). Extreme warm spells can have important societal consequences. The 2003 European heat wave claimed more than 70,000 human lives in Europe, including 15,000 in France, during the summer months. Between the 3rd and the 6th of August, unusually high mortality rates were observed in 12 European countries (Robine et al. 2008). Meanwhile, daily temperature records were broken over a large part of Europe. The observation dataset used in this paper indicates that the 2003 June–July–August (JJA) months experienced a larger number of warm records than any other months of the 1956–2005 period, as previously reported by Elguindi et al. (2012). This was also the only summer in which no new cold records were broken over France during fifty years of observations (Fig. 1). Barriopedro et al. (2011) estimated the 2003 and 2010 summers to be the warmest on record over ~25 % of Europe and show that the current summer record map of Europe has been marked by these two extreme summers. With our observations, we also estimate that more than 30 % of the European region experienced daily temperature records every day between the 5th and the 15th of August (not shown).

One advantage of using record-breaking events in assessing changes in extreme events is the independence of the probability of a record occurrence and the underlying distribution. Hence, different series of records can be compared whether or not they are characterized by the same probability density function. For a sequence of independent, identically distributed (iid) random variables (RVs) drawn from a continuous probability density, the probability for a record to occur at the n th time step after the initialization is $P_n = 1/n$. Such a sequence of RVs is often referred to as a stationary climate in the literature. A stationary climate can be defined simply as a climate in which no change in the shape of the temperature (and other variables) distribution can be found.

The theoretical results of records statistics were first used by Benestad (2003, 2004) to build a statistical model and detect higher number of observed warm events than expected from the hypothesis of iid RVs, or a stationary climate. Several studies have examined the case of a sequence of independent RVs in the presence of a linear trend to better represent the observed temporal evolution of temperature-breaking events (e.g. Redner and Petersen 2006; Newman et al. 2010; Wergen and Krug 2010; Franke et al. 2010; Wergen et al. 2014), or the case of sequences of RVs from distribution with increasing variance (Krug 2007).

There is a growing body of evidence suggesting that the hypothesis of a stationary climate cannot explain the observed increase or decrease in warm or cold temperature records, which have been found to be much higher or lower than expected in the last two decades. From European

stations, Wergen and Krug (2010) attributed 5 out of 17 daily temperature records per year to the warming climate. Trewin and Vermont (2010) found a 2–1 ratio of warm to cold records during the final years of the 1997–2009 period from Australian observations. From monthly observations, Coumou et al. (2013) showed that the number of maximum temperature records is now, on a global scale and despite large differences, on average five times larger than the expected number in a stationary climate.

Following a medium emission scenario (SRES A1B) for the twenty-first century, Meehl et al. (2009) projected with a climate model that the ratio of warm to cold records would increase from 2 to 1 at the end of the twentieth century to 50–1 at the end of the twenty-first century. Using the same emission scenario, an ensemble of 22 climate models and a global observation dataset, Ruokolainen and Räisänen (2009) found that by 2080 the maximum annual warm records could have been broken across 99 % of the surface of the globe. With an ensemble of five regional climate models, Elguindi et al. (2012) projected a value of ratio of several hundred by the end of the twenty-first century. Under a medium scenario (RCP4.5) Coumou et al. (2013) predicted the number of monthly heat records to be more than 12 times higher by the 2040s than expected globally in a climate with no long-term warming.

To summarize, different rates of increase of warm records or different ratio of warm to cold records can be found in the literature. Christiansen (2013) found a significant increase in the annual number of daily warm records over Europe in a reanalysis dataset, which is lost when considering individual seasons. Wergen et al. (2014) found that their statistical model is better appropriate for monthly than for daily temperatures over the US, because of a reduced variability. Hence, the effect of the warming on the occurrence of record events is controlled by a governing parameter: the ratio of the temperature change to the interannual standard deviation (Wergen and Krug 2010; Newman et al. 2010; Rahmstorf and Coumou 2011). Differences in the global warming pattern and in year-to-year variability suggest differences in the evolution of temperature record-breakings. Thus, the strongest and most statistically significant effects of warming are found in studies in which the data are monthly-to-annually averaged over large regions. The projections of temperature records must then be assessed at regional scales in order to better estimate the future extremes and better approach the adaptation to these events.

The important role played by changes in variance compared to changes in mean in assessing future extremes has been proven (Katz and Brown 1992) and evoked as a cause for the 2003 heat wave, for example (Schär et al. 2004). In addition to these studies focused on mean changes, Anderson and Kostinski (2010) developed a metric based on the

number of records and the reversibility in time to evaluate changes in interannual variability. Using a global (but mostly North American) ensemble of monthly time series of observations, they found a significant decrease in year-to-year variability of about -0.2 °C (over their 106 years of observations). Observations point to an increase in variability for the European summers in response to anthropogenic-induced warming (Scherrer et al. 2005; Parey et al. 2009), most specifically over central and eastern Europe (Della-Marta et al. 2007). On the other hand, observations show a decrease in year-to-year variability in winter (Scherrer et al. 2005; Parey et al. 2009).

In this paper, we mainly study daily temperatures from the E-OBS observations (Haylock et al. 2008) and an ensemble of simulations performed using the CNRM-CM5 model (Voldoire et al. 2012) to approach the following questions: Can the recent changes in observed record-breaking temperature be linked to the natural and anthropogenic forcings? How do the records evolve during the twentieth and twenty-first centuries? Are these evolutions comparable with one driven purely by internal variability? Do the model projections show any changes in interannual variability?

Section 2 introduces the datasets and the different methodologies developed in this paper. First, the past and future evolution of the mean annual number of temperature records is analyzed (Sect. 3). Then, Sect. 4 presents the projections of the seasonal evolution of records, as along with changes in interannual variability. Finally, we discuss and summarize our findings in the context of ongoing research in the field of temperature extremes and records (Sects. 5, 6).

2 Data and methods

2.1 Observed and simulated temperatures

Daily minimum and maximum observed temperatures (tasmin and tasmax) are taken from the European E-OBS version 9 dataset (Haylock et al. 2008). This dataset, on a half-degree regular grid, covers the time period from January 1950 to June 2013. The observed temperatures are interpolated on the model grid.

Simulated temperatures are taken from an ensemble of simulations from the CNRM-CM5 model (Voldoire et al. 2012). This model is used in the Coupled Model Intercomparison Project Phase 5 (CMIP5). Atmospheric fields (including tasmin and tasmax) are given by the atmospheric component (ARPEGE-Climat, v5.2) with a 1.4° horizontal resolution (both in latitude and longitude).

The control simulation (henceforth referred to as the CTRL simulation) is a long simulation (850 years of daily

data) in which all external forcings remain constant at their pre-industrial 1850 values. Non-physical long-term changes (model drift) can alter the estimates of the internal variability as well as the response to external forcings (Gupta et al. 2013). Therefore, we linearly detrend CTRL to remove spurious changes in daily minimum and maximum surface temperatures. Because CTRL also provides the initial conditions of the different historical simulations, the drift is removed from the historical simulations as well by a simple extrapolation of the appropriate CTRL drift.

A 10-member ensemble of historical simulations (HIST), forced by observed external forcings (natural and anthropogenic) over the 1850–2005 period, is used. In addition to HIST, two other single-forcing sets are also considered over the same period in order to isolate the effect of various external forcings. These attribution simulations use either all the natural forcings (solar activity and volcanic aerosols) or all anthropogenic forcings (greenhouse gases and aerosols), referred to as the NAT and ANT ensembles, respectively.

Three climate scenarios (Representative Concentration Pathways—RCP8.5, RCP4.5 and RCP2.6) based on different temporal evolutions of anthropogenic forcing are studied over the 2006–2100 period (van Vuuren et al. 2006, 2007). CNRM-CM5 has only one simulation for both RCP2.6 and RCP4.5, but an ensemble of five simulations for the RCP8.5 scenario (RCP8.5 ensemble from now on).

2.2 Calculation of temperature records

By definition, an upper or lower record is broken when a higher or lower value of maximum or minimum surface temperature appears in the annual time series, recorded after an initial date and dependent on the calendar day. As previously stated, for a sequence of iid RVs, the probability for a record to occur at the n th time step after the initialization is $P_n = 1/n$. The number of records is thus expected to decrease with n , the number of years from the initial date. This theoretical decay expresses the increasing difficulty for a record to break along the years if the climate can be viewed as a stationary random process (the dark grey line in Fig. 1). The probability P_n is commonly referred to in the literature as the record number expected in case of a stationary climate.

To assess the number of records and their evolution, we will either refer to the P_n form or its normalized nP_n variant, where the theoretical expected number of records is then 1. When comparing at a given time or period the number of observed and simulated records to the values expected in a stationary climate (meaning that their rate of change is then given by P_n), we will simply and systematically refer to the latter as “the expected record number”

instead of the longer expression “the expected record number in a stationary climate”.

We examine annual and seasonal temperature records by computing the sum of the record-breaking temperatures of all calendar days for the time period of interest. When examining European records, we analyze the sum of annual (or seasonal) records of all land grid points (defined by a land fraction >99 %). We do not initialize the records, so the first year presents the maximum number of records that can be broken. This is illustrated in Fig. 1, where the sum of the numbers of upper and lower records in summer over France decays from the initial value of 3036 (the number of grid points in France times the number of days in summer: 33×92), and then oscillates around the expected record number, according to year-to-year variability.

Note that to study the spatial distributions of the changes in records between two periods, we calculate temporal averages over 30 years. In this case and for the sake of clarity, we analyze the records under their normalized form to avoid the decrease in $1/n$. In addition, this decay is so abrupt that the use of a logarithmic scale is needed for plotting record evolutions, but such a scale compresses the highest values. This is not a problem for the lower records that decreases along the years, but it is with the increasing number of upper records, for which the normalized form is thus preferred. Hence, two different visualization forms for the upper and the lower records are used to better highlight their future evolution.

The minimum and maximum surface temperatures are correlated in both space and time. In order to fully respect the iid RVs case, our total number of time series would naturally be reduced if only independent time series were considered. Redner and Petersen (2006) performed statistical analyses to study the impact of the temporal correlation on the record statistics. They found that the day-to-day correlation does not affect the statistics of records calculated on a given calendar day (1 year apart), but they do affect the statistics of successive events, such as warm or cold spells. However, the temperature in a grid cell is correlated to its adjacent cells, and this spatial correlation must be taken into account when drawing conclusions about the statistical significance of the results.

The calculation of records is also dependent on the initialization. A particularly warm first year will, for example, imply that the following upper records will be harder to break. Elguindi et al. (2012) have developed a method to filter out the impact of the initialization, but we do not apply such diagnostics here. However, we have tested different initialization dates but did not find any significant differences in the mean evolution of records.

2.3 Assessing changes in record interannual variance

Throughout the century, a mean warming is projected over Europe, but it is very important to distinguish year-to-year changes from long-term changes. Here we study changes in interannual variance using the α parameter formulated by Anderson and Kostinski (2010). They developed a metric to examine the changes in variance in a time series from the statistics of records and the reversibility in time, without making any assumptions as to the underlying distribution. The authors defined their metric by the two following definitions: $\alpha = (UR_f - UR_b) + (LR_f - LR_b) = (UR + LR)_f - (UR + LR)_b$, with f and b signifying the forward and backward time direction and UR and LR the upper and lower records' number in the time series. Thus, a negative or positive value of $\langle \alpha \rangle$ (denoting the average of α over a region) indicates a negative or positive trend in variance, or decreasing or increasing interannual variability.

Anderson and Kostinski (2010) tested the metric on observed station data on global and monthly scales. Our objective is to assess the possible changes in the year-to-year variance of simulated minimum and maximum temperature records from 1956 to 2100. We first detrended the five simulations of that combined (HIST and RCP8.5) ensemble by removing a second order fit of the ensemble mean to each member, on all grid points and for all days.

2.4 Detection methodology

In a large number of previous studies, the changes in temperature records were detected using statistical models to estimate the internal variability of the considered temperature dataset. Meehl et al. (2009) used a bootstrap analysis within the observation dataset while Christiansen (2013) derived an ensemble of surrogates statistically identical to the observations with the trend removed.

In this paper, we estimate the internal variability using the long CTRL simulation over 850 years as well as the intra-ensemble variability of HIST simulations. This requires us to make the strong assumption that the internal variability of CNRM-CM5 is realistic, an assumption which is very difficult to verify as we do not have the observed counterpart. We will show that the total model variability is consistent with that of the observations regarding our analysis variables.

The first-order detection analysis is based on the following null hypothesis H_0 : *the evolution of temperature record is consistent with internal variability only*. A 90 % confidence interval (CI) of the record evolution under internal variability alone is built. Records were calculated in a large number of blocks from the CTRL and HIST set of simulations (the latter from which the ensemble mean was previously subtracted). The final number of blocks

necessarily depends on the length of the time series and varies from about 190 to 170 over the 1956–2005 and 1956–2100 periods, respectively. To increase the number of blocks in our sample, we use overlapping blocks. The blocks of 50 (145) years have a 40-year (140-year) overlapping period. The 90 % CI is then estimated from the record distribution. The upper and lower limits of the CI have also been smoothed by a 7-year running average for the sum of the number of annual records over Europe (15-year for other diagnostics). Note that the CI is not indicated at the beginning of the time series because the initial decay is steep and difficult to capture with a smoothing average.

The significance of the record changes can also be investigated on every grid cell, with regard to the corresponding limits of the CI. When considering a spatial analysis, the initial (and maximum) number of records is then reduced from the number of grid points multiplied by the number of days to the number of days only, this latter varying from 91 to 365 between seasonal and annual analyses. After 145 years of calculation, the lower limit of the CI is very often zero, thus biasing the analysis. Hence we can only estimate the significance of the changes for the upper records, not for the lower records (which decrease during the twenty-first century).

To counter this limitation, we use a different approach based on the number of zero-record occurrences, calculated in the ensemble of blocks used to build the CI. The number of blocks in which no lower records are broken during the 30-year period of consideration is calculated for every grid cell and then spatially averaged over Europe. This gives us an indication of the mean number of blocks over Europe that experienced a zero-record occurrence in 30 years. We will refer to this metric as CTRL-zero in this paper.

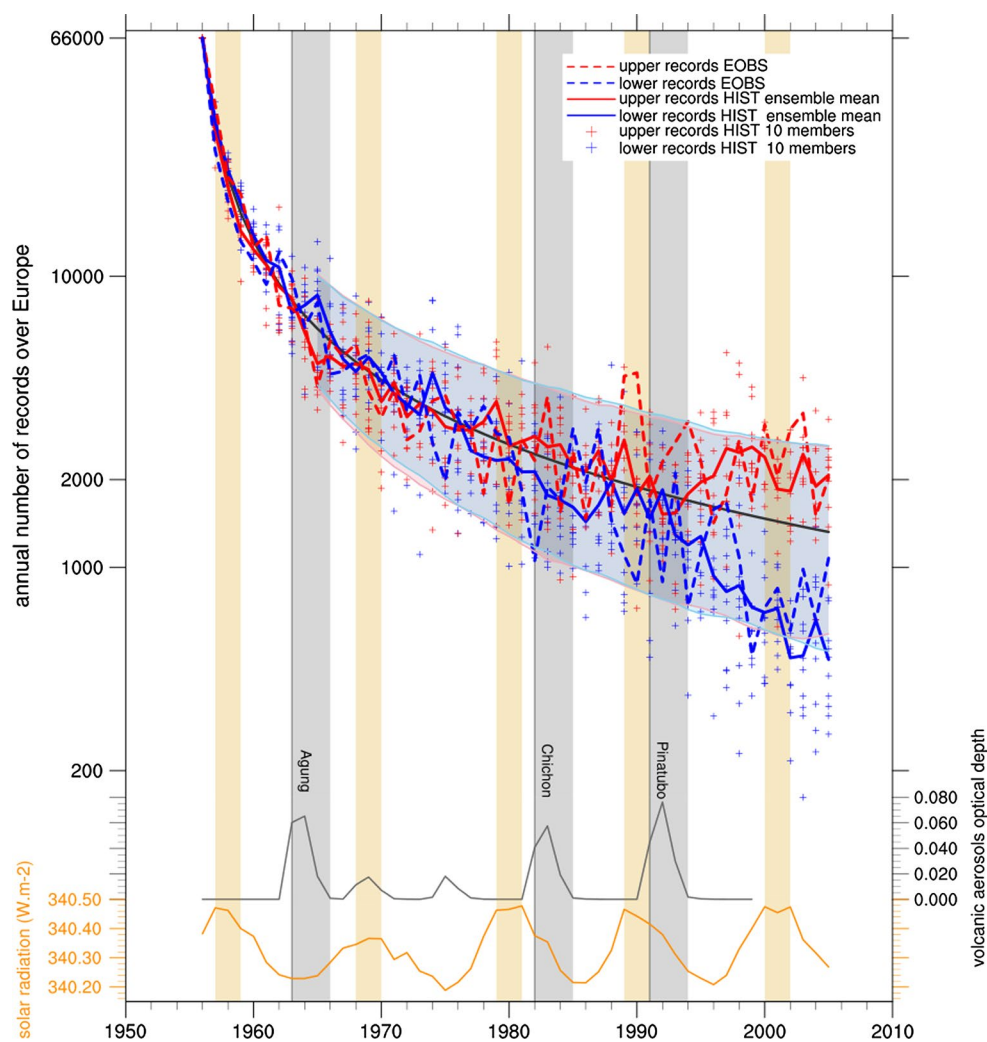
The detection of changes in interannual variability from 1956 to 2100 is also assessed through the following null hypothesis $H_0 : \alpha = 0$. The α parameter for both *tasmin* and *tasmax* is calculated for the ensemble of blocks from the CTRL simulation, and in every grid cell. A 90 % CI can then be estimated from this set of α values.

3 Annual analyses

3.1 Historical period (1956–2005)

First, the simulated annual numbers of upper and lower records are compared to the observations over the second half of the twentieth century (1956–2005; Fig. 2). As previously mentioned in the literature, the observed annual numbers of records follow the decay in $1/n$. Until the 1980s, they oscillate around the expected record number, according to interannual and decadal variability. From the

Fig. 2 Evolution of the annual number of upper (red) and lower (blue) records summed over Europe in the observations (dashed lines), the ensemble mean (solid lines) and the ten members (crosses) of the HIST simulations, from 1956 to 2005. The record evolution expected in a stationary climate is represented by the dark grey line. Shaded areas correspond to the 90 % confidence interval, due to internal variability, of the upper (pink) and lower (light blue) records. The two bottom curves illustrate the observed evolutions of natural forcings. The volcanic aerosols optical depth (grey) is averaged over the northern hemisphere. Three major eruptions are notified by vertical grey lines and the volcano's name. The solar radiation at the top of the atmosphere is drawn in orange. Caution needs to be taken with the logarithmic scale of the Y-axis



1960s to the mid-1970s, we observe a cold period with a much higher occurrence for the lower than for the upper records, which is then followed by a warmer period. Starting at the beginning of the 1990s, we observe an increasing or decreasing annual number of upper or lower records that seems to deviate from the stationary climate behavior in agreement with previous studies (Wergen and Krug 2010; Meehl et al. 2009; Wergen et al. 2014; Elguindi et al. 2012).

This change in the evolution of records since the 1980s could be explained by the global dimming and brightening suggested by Wild (2011). From the 1950s to the 1980s, an increasing concentration of anthropogenic aerosols partially compensated for the effects of the greenhouse-gas-induced warming. Since then, industrial aerosol emissions have decreased across Europe and so the solar surface radiation has increased, contributing to a more efficient warming.

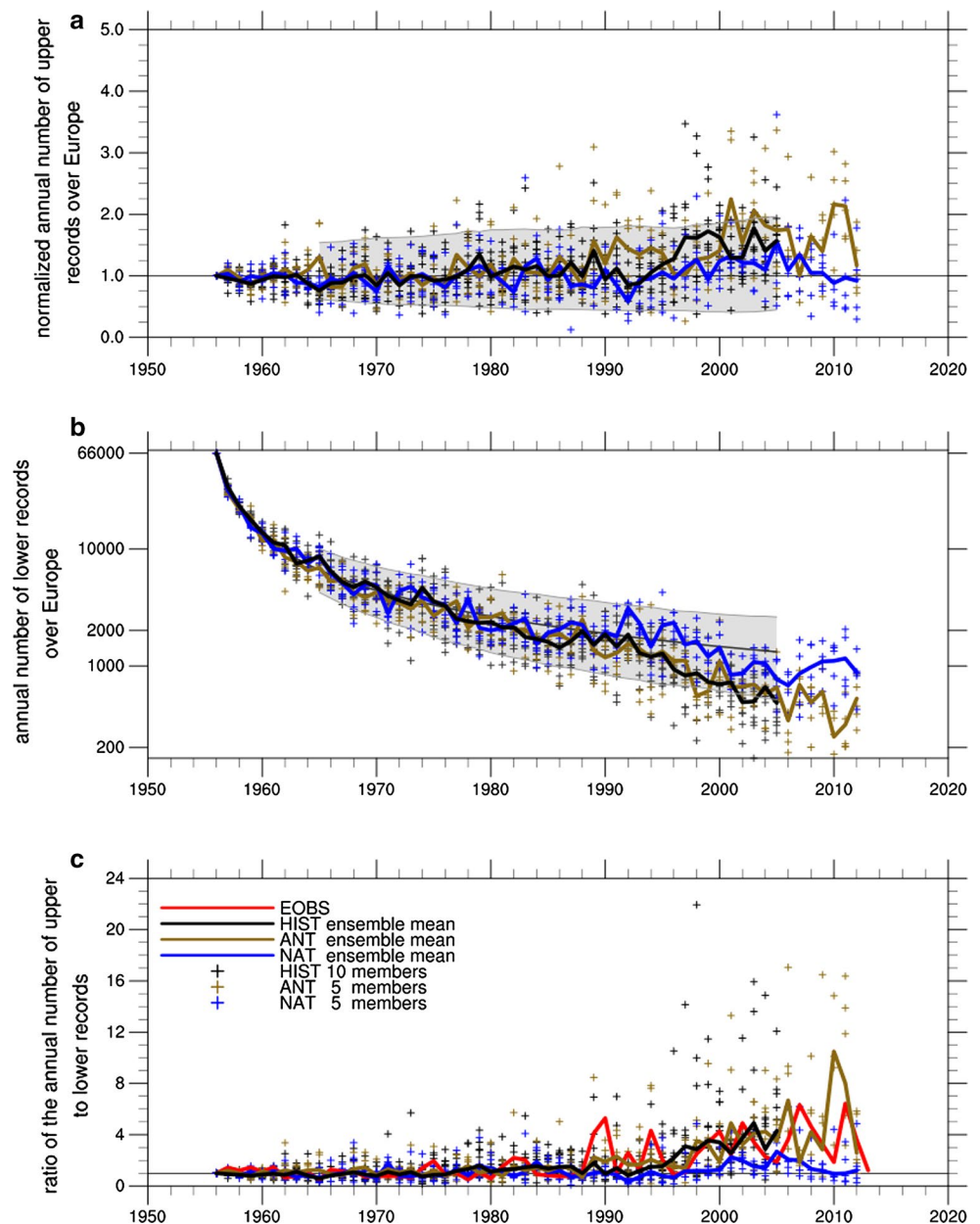
As expected, the observations are noisier than the HIST ensemble mean, yet the model is capable of reproducing the slowly varying part of the observed evolution of both

upper and lower records (Fig. 2). The spread of the HIST simulations seems realistic in comparison with the intensity of an observed peak. The ratio of upper to lower records stays around 1 in both the observations and the model until the end of the 1980s, when it increases to about 4–1 (Fig. 3), as found in Elguindi et al. (2012) using the same observation dataset.

The member's record evolution (Fig. 2) suggests that the observed and simulated interannual variability do not significantly change during this period. The apparent increase of interannual variability from the ratio analysis (Fig. 3c) present at the end of the period should not be interpreted as a real signal, as it is likely due to the low rate of occurrence of lower records. Hence, with the decreasing tendency of the number of lower records, the ratio analysis does not appear optimal for describing the future evolution of the records: as the denominator tends to zero, the ratio can easily reach very large values.

From 1956 to the end of the 1980s, the evolution of observed and simulated records does not clearly emerge

Fig. 3 Evolution of the annual number of upper (a) and lower (b) records summed over Europe and the ratio of these two (c) in the observations (red line), the ensemble mean (solid lines) and the members (crosses) of the HIST (black), ANT (brown) and NAT (blue) simulations, from 1956 to 2005. Records in ANT and NAT ensembles were integrated for a slightly longer period (up to 2012) than in HIST simulations. Upper records are under the normalized form. The record evolution expected in a stationary climate is represented by dark grey lines. Shaded grey areas correspond to the 90 % confidence interval due to internal variability. Caution needs to be taken with the logarithmic scale of the Y-axis in b



from internal variability estimates. Thereby we cannot reject the null hypothesis for either the observations or the model. Even though we observe a deviation from the stationary climate behavior starting at the end of the 1980s, the simulated and observed changes are still within the range of the model's internal variability until the end of the twentieth century.

Three major eruptions occurred from 1956 to 2005 (Fig. 2). The Agung volcano, which caused the weakest eruption of this period, does not seem to have influenced the records. Shindell and Schmidt (2004) show that major eruptions such as those of El Chichon and Mount Pinatubo result in contrasted seasonal signals on European temperatures. Here, it is difficult to conclude a significant

influence of these two eruptions on the annual number of temperature records, despite the visible decrease and increase in the number of lower and upper records the year of the El Chichon eruption and the year following the eruption of Mount Pinatubo, which became active in June 1991. In addition, the temperature anomalies associated with the variations induced by El Niño/Southern Oscillation (ENSO) can mask the volcanoes' impact on the evolution of temperature records (Wigley 2000). Finally, the evolution of both the upper and lower records does not appear to be significantly influenced by variations in solar activity. Indeed, positive or negative phases of the solar cycle do not induce higher or lower occurrences of records.

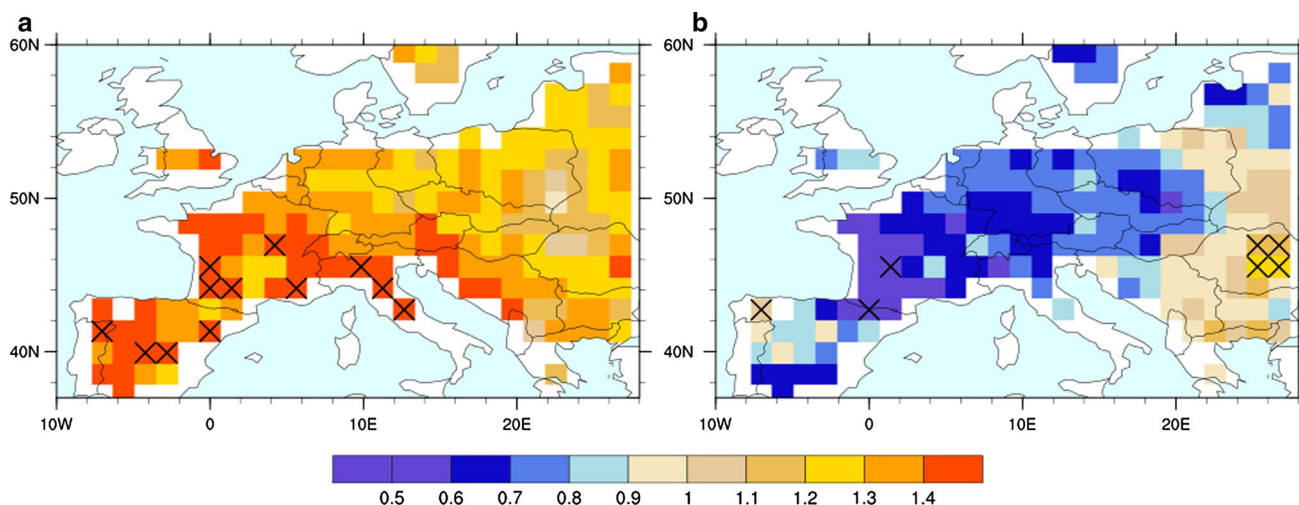


Fig. 4 Spatial distribution of the annual number of upper (a) and lower (b) records in the observations, averaged over the 1976–2005 period. Crosses indicate grid points where the observed values are outside the 90 % confidence interval which represents the HIST

The spatial distribution of the records from the HIST simulations and the observations are compared in Fig. 4. The observations are within the model distribution almost everywhere in Europe for both records, except for a few (<10 %) grid cells. We conclude that the model is capable of reproducing a spatial distribution of the records comparable to that of the observations.

Moreover, in comparison with the expected record number, we can observe an increase in the mean number of upper records over almost all of Europe, and a decrease in the number of lower records in the central part of the domain. This is the result of the previously mentioned warming trend from the beginning of the 1980s. Indeed, maps of records averaged over the 30-year period before the 1980s present values close to the expected record number.

3.2 Simulations with single forcings

We now use ensembles of attribution simulations to link the present-day evolution of the records to the natural and anthropogenic forcings. Figure 3a, b presents the evolution of the upper and lower records in the ANT and NAT ensemble means up to 2012 (as they were integrated for a slightly longer period than the HIST ones), in comparison with the HIST ensemble mean.

From 1956 to the beginning of the 1980s, the three ensemble means are very similar for both the upper and lower records, which is reflected in the mean ratio of about 1 (Fig. 3c). Since the 1980s, the upper records in the NAT ensemble mean continue to oscillate around the expected record number. Meanwhile, the number of upper records in the ANT ensemble mean is higher and closer

ensemble mean ± 1.64 times the intra-ensemble standard deviation. Records are under the normalized form, where the expected record number in a stationary climate is 1

to that of HIST, with the presence of a positive trend. The lower records in the NAT ensemble mean are also closer to expected record number than the HIST ensemble mean, unlike the ANT ensemble mean. These differences in the evolution of records between these two ensembles are well illustrated by the ratio of upper to lower records (Fig. 3c). The ANT and HIST ensemble means are much closer to each other and to the observations.

Averaged over Europe, the mean number of upper and lower records in NAT ensemble is very close to the expected record number, but this is not the case in the HIST ensemble (Fig. 5). The higher and lower occurrences of upper and lower records previously observed in the temporal evolutions are rather homogeneous over the region. The ANT simulations are also capable of reproducing these changes, even if the maxima and minima are not exactly collocated. Note that we do not expect similar patterns between HIST and ANT due to internal variability and natural forcing effects.

Unlike ANT, the NAT ensemble does not appear capable of reproducing either the temporal or spatial distribution of the HIST ensemble records. However we cannot strictly attribute the evolution of the records during the late twentieth century to anthropogenic emissions. According to our detection test, the observed and simulated record evolutions are still within the range of the internal variability. Yet, the HIST and ANT ensemble means are very close to the limits of the CI at the end of the period as a result of the ongoing warming trend (particularly true for the lower records). Additionally, the number of the records in these two ensembles at the end of the twentieth century seems to differ from the expected record number, unlike in the NAT ensemble.

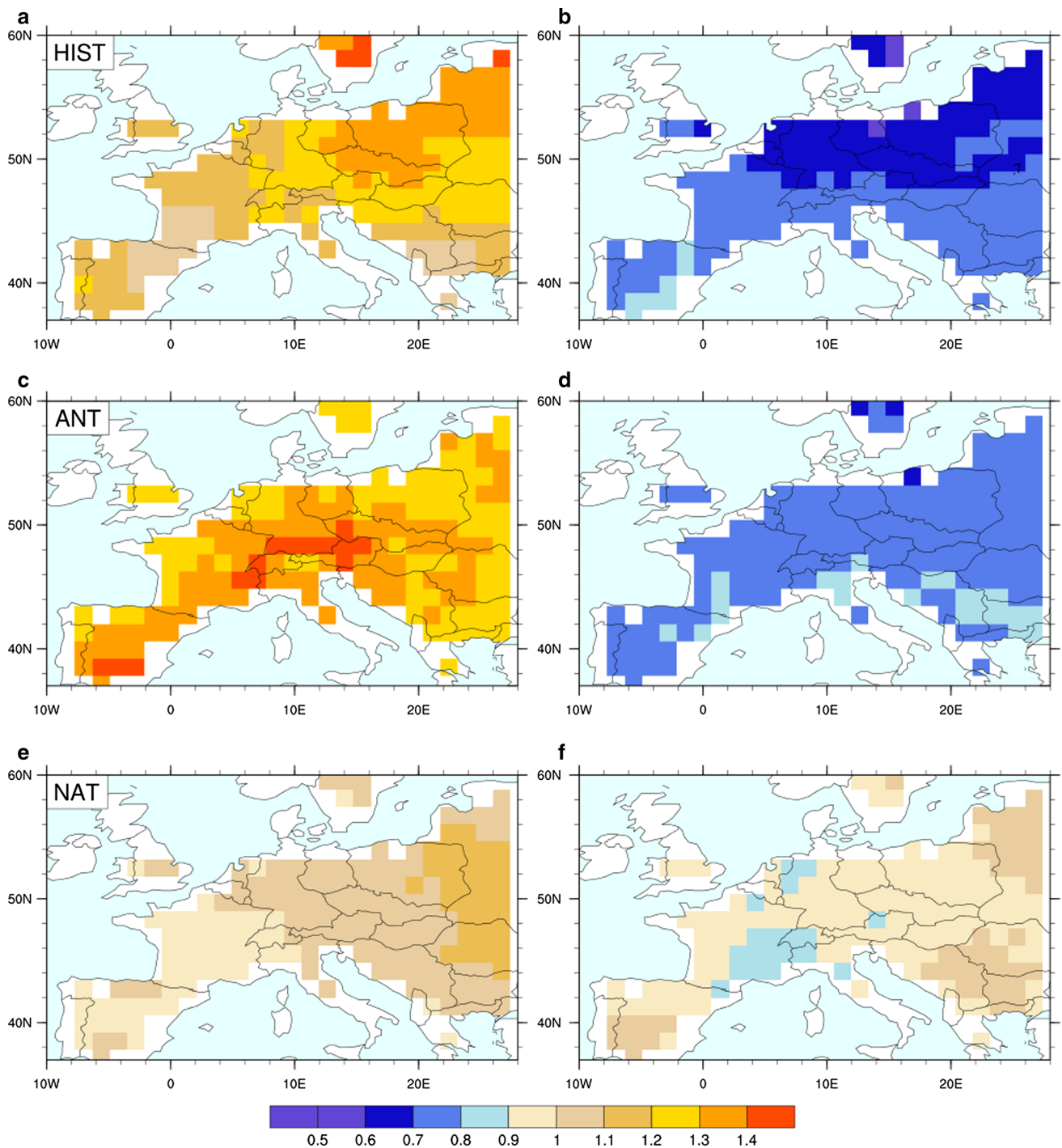


Fig. 5 Spatial distribution of the annual number of upper (a, c, e) and lower (b, d, f) records averaged over the 1976–2005 period in HIST (a, b), ANT (c, d) and NAT (e, f) ensemble means. There are no sig-

nificant results at the 10 % level. Records are under the normalized form, where the expected record number in a stationary climate is 1

3.3 Future period (2006–2100)

Until the 2020s, the evolution of records under the three scenarios is quite comparable (Fig. 6). The 90 % CI for both types of record does not significantly widen with time,

and here we can easily conclude that significant changes are detected.

We first focus on the RCP8.5 scenario. The current observed emissions of CO₂ are actually still higher than those established in this scenario (Peters et al. 2012). From the

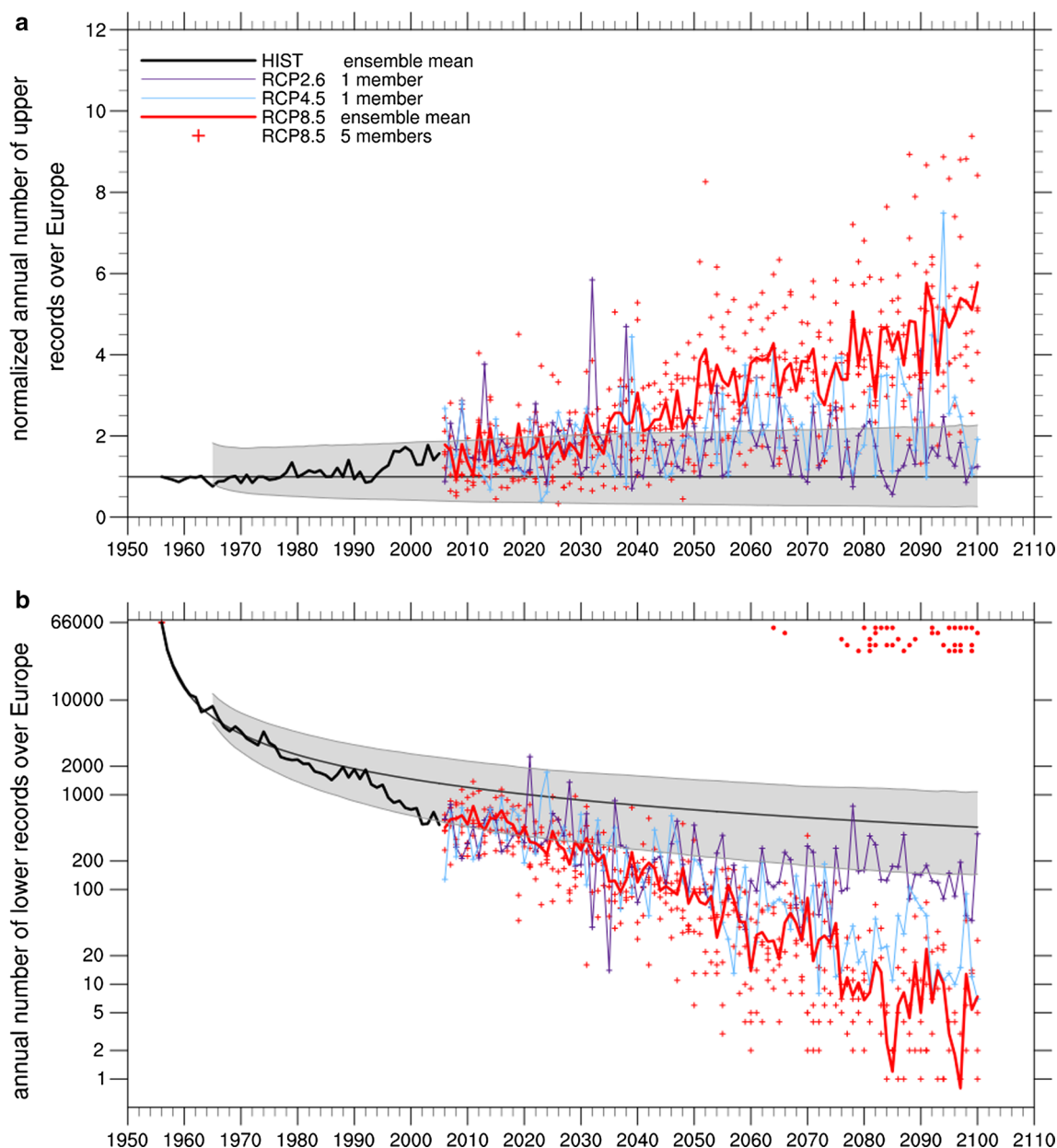


Fig. 6 Evolution of the annual number of upper (a) and lower (b) records summed over Europe in the ensemble mean (solid lines) and the members (crosses) of HIST (black), RCP2.6 (purple), RCP4.5 (cyan) and RCP8.5 (red) simulations, from 1956 to 2100. Upper records are under the normalized form. The record evolution expected

in a stationary climate is represented by dark grey lines. Shaded grey areas correspond to the 90 % confidence interval due to internal variability. Dots notify years of zero-record occurrences over the entire European domain, one line per member. Caution needs to be taken with the logarithmic scale of the Y-axis in b

2020s onwards, a clear warming trend is present in the upper and lower record time series (Fig. 6). At the end of the twenty-first century, the projected number of upper records in the RCP8.5 ensemble rises to about 5 times the expected record number, whereas the projected number of lower records is less than 10 compared to an expected one of several hundred.

From the 2060s, the model simulates years with no lower record occurrences (in any of the 181 grid cells and any of the 365 days). The ensemble mean is outside the

range of internal variability from the 2030s for the upper records, and from the 2020s for the lower records. Hence, we detect significant changes in the annual evolution of the European upper and lower records beginning in the 2030s and the 2020s, respectively.

The maps of Fig. 7 present the annual numbers of upper and lower records for the RCP8.5 ensemble means, averaged over 2 periods of 30 years and compared to the expected record number (here 1).

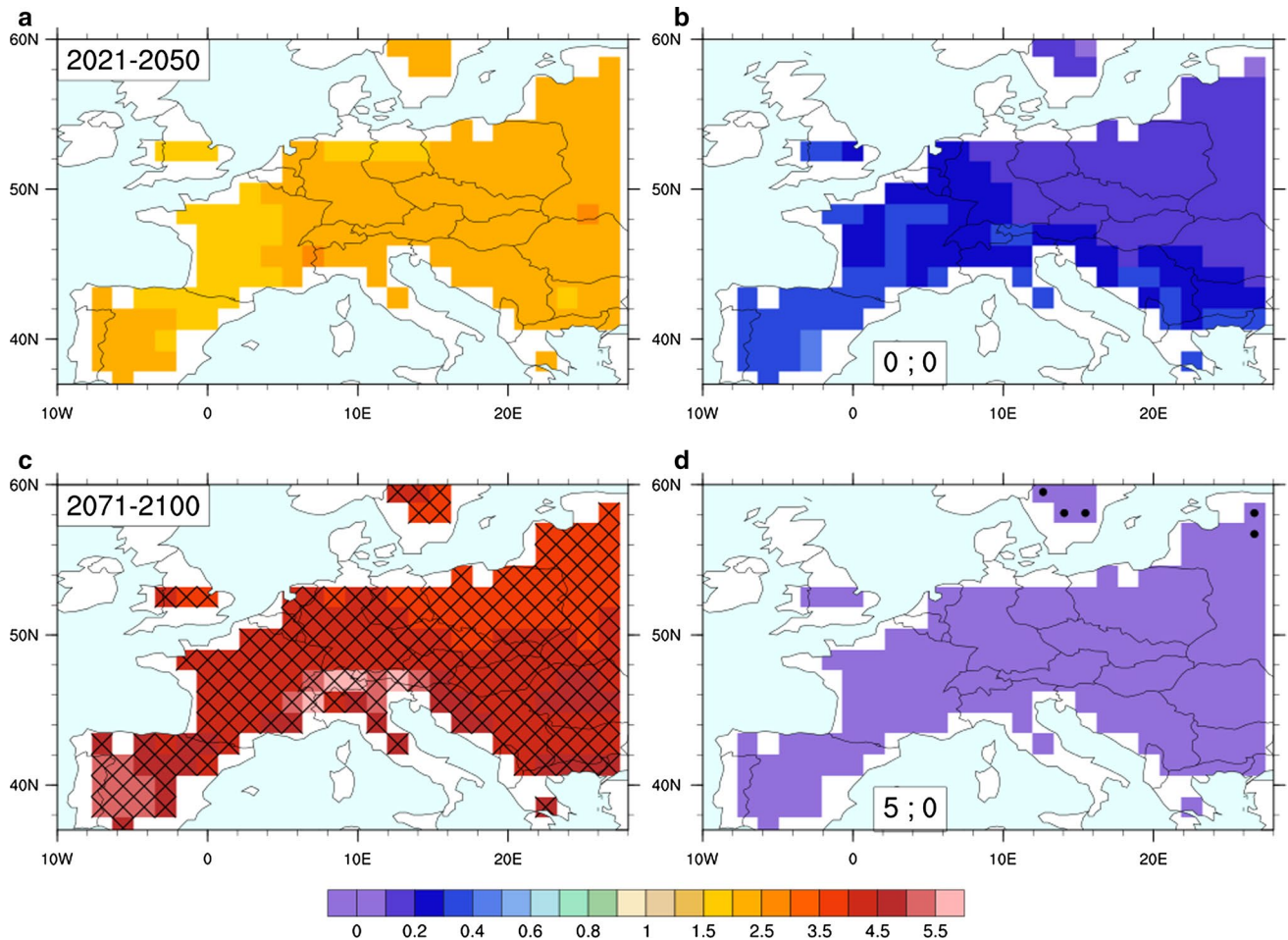


Fig. 7 Spatial distribution of the annual number of upper (a–c) and lower (b–d) records averaged over the 2021–2050 (a, b) and the 2071–2100 (c, d) periods, in RCP8.5 ensemble mean. *Crosses* indicate grid points with significant results at the 10 % level. Records are under the normalized form, where the expected record number in a

stationary climate is 1. *Dots* indicate grid points of zero-record occurrences over the entire 30-year period and for the five simulations of the ensemble. The first number in the box corresponds to the total number of zero-record occurrences in the ensemble mean, the second is CTRL-zero

The first period (2021–2050) characterizes the mid-century future climate. The deviation from the stationary climate, seen in the spatial distribution of the HIST ensemble means (Fig. 5), intensifies until 2050. The mean number of annual upper records is between 2 and 3 times the expected record number. The mean numbers of annual lower records fall to 0.1 and 0.3. However, we do not find any statistically significant changes, and the spatial patterns are quite homogeneous.

At the end of century, the mean number of annual upper records rises to 5.5. The upper records indicate a more significant warming in southern Europe, with values higher than 5 in Southern Spain and in the Alpine region. Using an ensemble of RCMs, Elguindi et al. (2012) also found a higher number of upper records around the Mediterranean, the Iberian Peninsula and France. In contrast with the previous period, statistical significance is reached for all grid points.

As for the lower records, the mean annual number falls close to zero, indicating that only a few records were established during these three decades. Meanwhile, 5 zero-record occurrences are found in northern Europe, which shows that during this 30-year period, no lower record occurs on any of the 365 calendar days among the 5 members. In comparison, CTRL-zero is exactly equal to zero, indicating that in the ensemble of blocks used to build the CI, there are no zero-record occurrences in a 30-year period.

It is interesting to note that, under all three scenarios, the upper and lower records are almost always above and below the expected record number (Fig. 6). Thus, the warming trend initiated in the 1980s in the HIST ensemble mean is projected to impact the evolution of records throughout the twenty-first century. Under the RCP2.6, this results in an evolution of records inconsistent with that of a

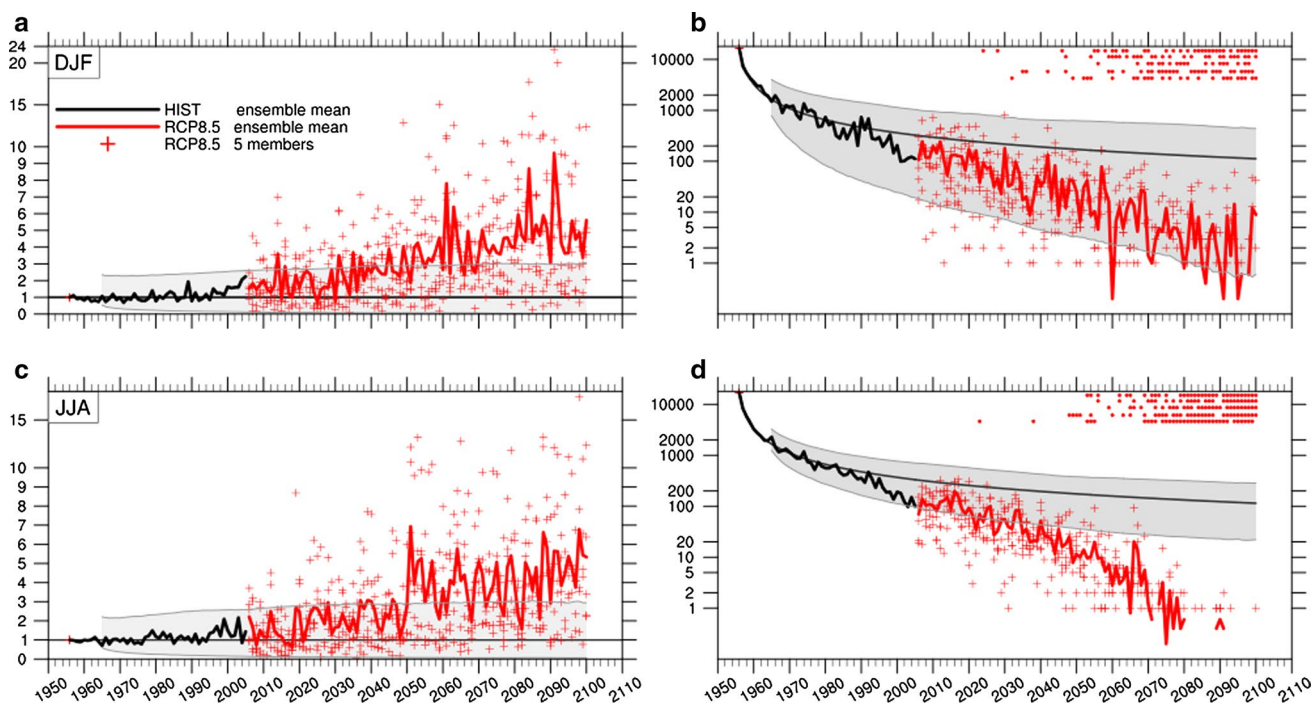


Fig. 8 Evolution of the seasonal number of upper (a–c) and lower (b–d) records summed over Europe in the ensemble mean (solid lines) and the members (crosses) of HIST (black) and RCP8.5 (red) simulations, in winter (a, b) and summer (c, d), from 1956 to 2100. Upper records are under the normalized form. The record evolution expected in a stationary climate is represented by dark grey lines.

Shaded grey areas correspond to the 90 % confidence interval due to internal variability. Dots notify years of zero-record occurrences over the entire European domain, one line per member. Caution needs to be taken with the nonlinearity (a–c) and the logarithmic scale (b–d) of the Y-axis

stationary climate, even if the evolution appears quite stable. Indeed, the evolution of upper records is mostly contained within the CI, but this is less evident for the lower records. This scenario presents the lower and even decreasing emissions of greenhouse gases over the course of the twenty-first century. Yet, the evolution of the records (and the lower records in particular) do not appear consistent with internal variability.

During the first half of the twenty-first century, the projected evolution of both upper and lower records is quite comparable between RCP2.6 and RCP4.5. Then, a pronounced warming trend appears under RCP4.5, which is particularly noticeable in the evolution of lower records. From the beginning of the 2040s, the lower records under this medium scenario evolve outside the CI. This is less evident for the upper records, whose evolution is very noisy due to year-to-year variability.

While it is difficult to claim detection of record change under RCP4.5 relying on a single member, the projected evolution of the upper and lower records seems barely compatible with the internal variability of the model in the second half of the century. This result is broadly consistent with those of Meehl et al. (2009) using a roughly similar greenhouse gas scenario. With one simulation, they also found an

impact of the warming trend on the number of records, along with a deviation from the stationary climate that began in the 1980s and intensifies during the twenty-first century.

4 Seasonal analyses

4.1 Mean evolution of the records

Here we mostly focus on the winter and summer seasons. When necessary, we simply mention in the text some of the results related to spring and autumn. First, we note that the null hypothesis cannot be rejected at the 10 % level over the second half of the twentieth century (Fig. 8). Thus, the simulated seasonal changes in records (like the annual changes) are always within the range of internal variability, with no compensation between seasons.

We first focus on the changes of upper records and compare the projected number of records to the expected record number. Note again here that this number is 1 when we use the normalized form to estimate the expected number of records (Fig. 8a–c).

In winter, the RCP8.5 ensemble mean of upper records presents a largely linear increase from the 2020s to the

end of the century, with significant results from the 2040s onwards. In the last three decades of the twenty-first century, the mean number of records is projected to reach values around 5, with mean values between 3 and 10 times higher than the expected record number. Statistical significance for the autumn changes is reached a decade later than in winter but several decades earlier than in spring.

In summer, an abrupt change in the middle of the century seems to separate the projections of the twenty-first century into two distinct phases, with a very slow increase during the first and an abrupt rise followed by a plateau in the second. This is likely due to sampling as only one of the five members presents a very abrupt peak that dominates the ensemble mean. By 2100, the mean number of records in summer is projected to rise up to about 5, with mean values between 2 and 7 times higher than the expected record number for the second half of the twenty-first century.

Like the annual projections, the seasonal projections present a significant continual decrease of lower records beginning in the 1980s (Fig. 8b–d). This behavior can also be seen in the zero-record occurrences. Independently of the season, zero-record occurrences first occur in the 2020s and become more numerous in the last four decades. Consequently, the seasonal numbers of records present a substantial decrease compared to the expected record number, here about one hundred at the end of the twenty-first century.

Contrary to the upper records, we do find a season where no significant changes are identified over the future period. Indeed, the evolution of lower records in winter is mostly included in the CI. It is interesting to note that the winter CI is the widest of the four seasons, with a lower limit close to 0. By 2100, the mean number of lower records in winter is projected to decrease to about 2, with annual values remaining inferior to 20 in the last 30 years of the twenty-first century.

The decrease in lower records is significant beginning in the 2030s in autumn, and the 2050s in spring. The changes in lower record are even more intense when considering the summer season, which presents a significant decrease in record occurrences beginning in the 2020s. Once again, it is interesting to note that summer is the season with the narrowest CI. In the last two decades, there are almost no record occurrences in any of the five members, any of the summer days and any of all grid points of Europe. This result is highly significant and reveals the impact that climate change could have on lower records, or on the nighttime temperature in summer.

Maps of mean numbers of upper and lower records are presented only for the last 30 years of the twenty-first century (Fig. 9), and the projected numbers of records are compared to the expected record number (here 1 again). Note that as with the results from annual projections (Fig. 7),

no significant results are found in any earlier periods (not shown).

In winter, about 50 % of the European domain experiences a significant increase in upper records, between 3.8 and 7.1 times the expected record number, mostly in northeastern and central Europe and the Alpine region. The maximum increase occurs over the Alps, with values up to 7 times the expected record number.

The summer season shows a very different pattern, with significant results gathered around the Mediterranean Sea and a maximum increase greater than 6. Unlike during winter, northern Europe presents a smaller, insignificant increase. The autumn pattern captures the transition between the contrasting summer and winter patterns, whereas the spring season shows the smallest increase in upper records among all seasons.

These contrasted spatial patterns are not found on the map of lower records. Indeed, the spatial distributions of lower records show quite similar results between all seasons and the annual distribution. A homogeneous mean number of lower records of about 0.1 is found, with almost no records occurring over Europe during the last 30 years of the twenty-first century. A minimum decrease can be found in a few points near the Mediterranean Sea in winter, with values up to 0.18.

However, the zero-record occurrences show some contrasted patterns between the seasons. In winter, a large number of zeros are gathered in northeastern Europe, whereas in summer, the zeros cover more than 70 % of Europe, especially in the eastern region. The total number of zero-record occurrences in the ensemble mean is compared to the CTRL-zero number, which is extremely low. Consequently, we find a large statistically significant decrease in lower record occurrences for the four seasons.

Winter and summer patterns bring to mind spatial structures commonly found in studies focused on mean changes in surface temperatures over Europe. Using a multi-model approach from a large ensemble of CMIP5 models, Terray and Boé (2013) highlighted a southwest–northeast gradient in winter with a maximum warming of 8 °C over northeastern Europe. A minimum increase of 2.5 °C occurs over the Atlantic coast, protected by the westerly flow and a larger land–sea thermal contrast. In summer, a meridional gradient is found, with maximum values of 8 °C around the Mediterranean edge, compared to the beginning of the twentieth century.

These contrasted patterns are explained by different mechanisms. In winter, the temperature–snow albedo feedback explains the warming over regions where the snow cover is projected to decrease during the century. In summer, the warming is mainly controlled by land–moisture–atmosphere interactions. The evapotranspiration over the Mediterranean land region is limited by the soil moisture, but the soil moisture

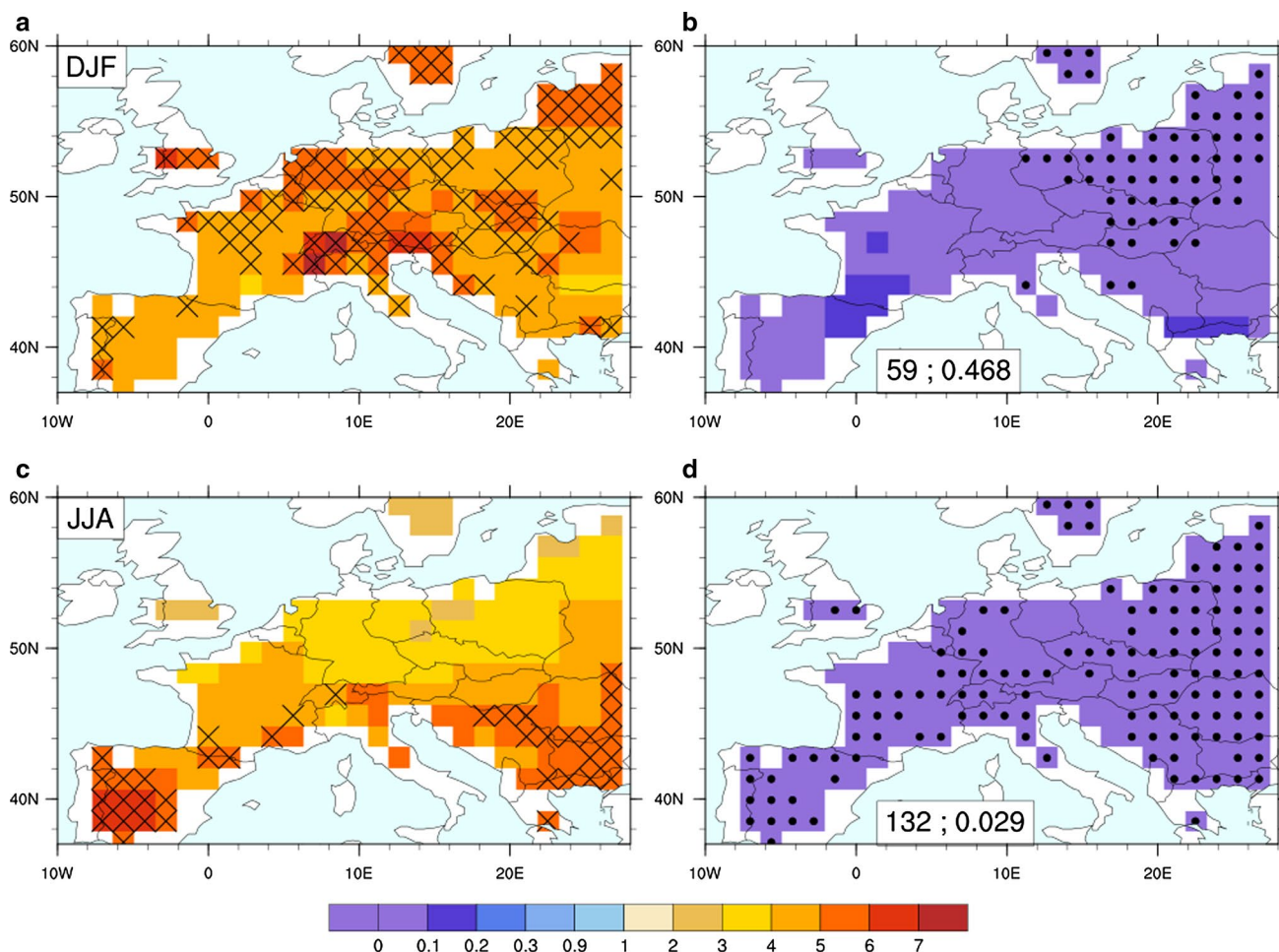


Fig. 9 Spatial distribution of the seasonal number of upper (a–c) and lower (b–d) records averaged over the 2071–2100 period in RCP8.5 ensemble mean, in winter (a, b) and summer (c, d). *Crosses* indicate grid points with significant results at the 10 %. Records are under the normalized form, where the expected record number in a stationary

climate is 1. *Dots* indicate grid points of zero-record occurrences over the entire 30-season period and for the five simulations of the ensemble. The first *number* in the *box* corresponds the total number of zero-record occurrences in the ensemble mean, the second is CTRL-zero. Caution needs to be taken with the nonlinearity of the color scale

content is projected to decrease (Boé and Terray 2008) along with the cloud cover (less evaporation). In response to the enhanced radiative flux at the surface (due to less clouds), an increase in sensible heat compensates for the limited latent heat and ultimately causes a warming at the surface.

4.2 Changes in record interannual variance

The different widths of the CIs show that the model's internal variability amplitude has a strong seasonal dependence (Fig. 8). The winter season has the largest one, and no significant changes in lower records are found in this season despite a substantial decrease. On the contrary, the lower record evolution first leaves the range of the internal variability in summer, where it is the smallest.

The largest contribution to internal variability comes from interannual time scales rather than lower frequencies.

This year-to-year variability is also noticeable throughout the projection ensemble spread. For example, the number of upper records during the last 30 winters of the twenty-first century in the ensemble mean is about 5, but meanwhile the 5 members indicate values between 0 and 24 (Fig. 8a). As expected, the RCP8.5 ensemble spread indicates greater interannual variability in winter than in summer, with that of spring and autumn lying in between (not shown). At the end of the twenty-first century, despite the projected large increase in mean, the internal variability could still induce years with few record occurrences as well as years with more than 20 times the expected record number. This is also reflected in the ratio of the long-term trend to the short-term standard deviation, which has been shown to control the increase in warm records (Wergen and Krug 2010; Newman et al. 2010; Rahmstorf and Coumou 2011).

The previous figures could give some clues as to the possible changes in variance along the twenty-first century, but caution must be taken with such analyses. The interannual variability seems to increase in both annual and seasonal analyses (Figs. 6, 8).

Using the α parameter, we examine the changes in interannual variability in the RCP8.5 ensemble from 1956 to 2100, independently from the long-term changes (Fig. 10). Considering annual analyses averaged over Europe for both daily minimum and maximum surface temperatures, we find $\langle\alpha\rangle$ values close to zero. Thus, no change in variance would occur over this period.

But the spatial distributions of α show that this is due to compensations between two opposite patterns. The domain is divided in two, along a southwest–northeast gradient. Because of these spatial compensations, we find values of $\langle\alpha\rangle$ statistically significant only for the maximum temperatures in summer and the minimum temperatures in winter. However, the spatial distribution of α still indicates large areas of significant values elsewhere. This illustrates the limitations of the use of $\langle\alpha\rangle$.

We now focus primarily on the spatial distribution of α in winter and summer, as annual analyses present a mixing of the signals of these two strong seasons. Spring and autumn show the same transition gradient, with positive values in southwestern Europe and negative values in northeastern Europe (not shown).

In winter, a negative trend in variance is found for both the minimum and the maximum surface temperatures over Europe, with significant values gathered over northeastern Europe. This result appears stronger for the minimum temperatures, with negative values statistically significant over three quarters of the domain.

In summer, maps of α are homogenous over Europe (although not significant everywhere) and show a positive trend in variance for both minimum and maximum temperatures. This increase is particularly pronounced over France and northern Spain for the maximum temperatures.

The decrease in winter appears greater than the increase in summer. Schär et al. (2004) and Seneviratne et al. (2006) have highlighted an increase in the year-to-year variability of the summers over central and eastern Europe in response of the warming induced by greenhouse gases. This change in the variability of the European summer is also found by Fischer et al. (2012), when considering only models with interannual variability correctly simulated at the present time, but with an increase found further south.

5 Discussion

From an ensemble of simulated daily data and daily observations, we have shown that the current number

of warm temperature records is still within the range of the internal variability of the CNRM-CM5 model. Using a set of monthly and global observations, Coumou et al. (2013) show that the current number of warm records is already on average five times higher than in a stationary climate with no long-term warming. Hence, a much more pronounced signal can be found in other studies examining monthly-to-seasonally averaged data and/or spatial averages over large regions. In such cases, the ratio of the long-term warming trend to the interannual standard deviation is increased, as is the number of warm records. This reflects the high sensitivity of the record evolution to temporal and spatial scales. Further, distinctions between models can also explain differences in the evolution of records. Thus, studies evaluating the evolution of record-breaking temperatures in the same region might have different results if based on data with different temporal scales. From daily data, the significance of the results is also harder to obtain when considering regional domains such as Europe, particularly for seasonal analyses (Christiansen 2013).

Consequently, a quantitative comparison of our results to those of previous studies is difficult, but a qualitative assessment highlights common findings. From the 1980s onwards, we found an observed and simulated deviation of the records from the stationary climate that characterized the 1960s and 1970s, in agreement with previous studies (Wergen and Krug 2010; Meehl et al. 2009; Elguindi et al. 2012; Wergen et al. 2014; Coumou et al. 2013). This deviation consists of an increasing number of upper records accompanied by a decreasing number of lower records. All studies also project this change in the evolution of records to be accentuated over the course of the twenty-first century. Few studies have investigated the spatial distribution of these changes. With regard to the future seasonal number of records, we show that the Mediterranean region is particularly affected in summer, whereas central and northeastern Europe is more impacted in winter. These results are consistent with the findings of Elguindi et al. (2012) based on regional climate models.

Southern Europe and the Mediterranean basin are projected to be strongly affected by an important increase in the number of warm records in summer (Fig. 9). Here we discuss the main physical processes responsible for the changes in extreme warm temperatures in summer in this sensitive region. The evolution of a set of surface variables related to soil–moisture interactions and clouds processes averaged over southern Europe is now investigated. We do not evaluate the possible contribution of the large-scale circulation, although it can also play an important role in the surface temperature warming. Changes in large-scale circulation have smaller signal-to-noise ratios and would require a larger ensemble to be properly assessed.

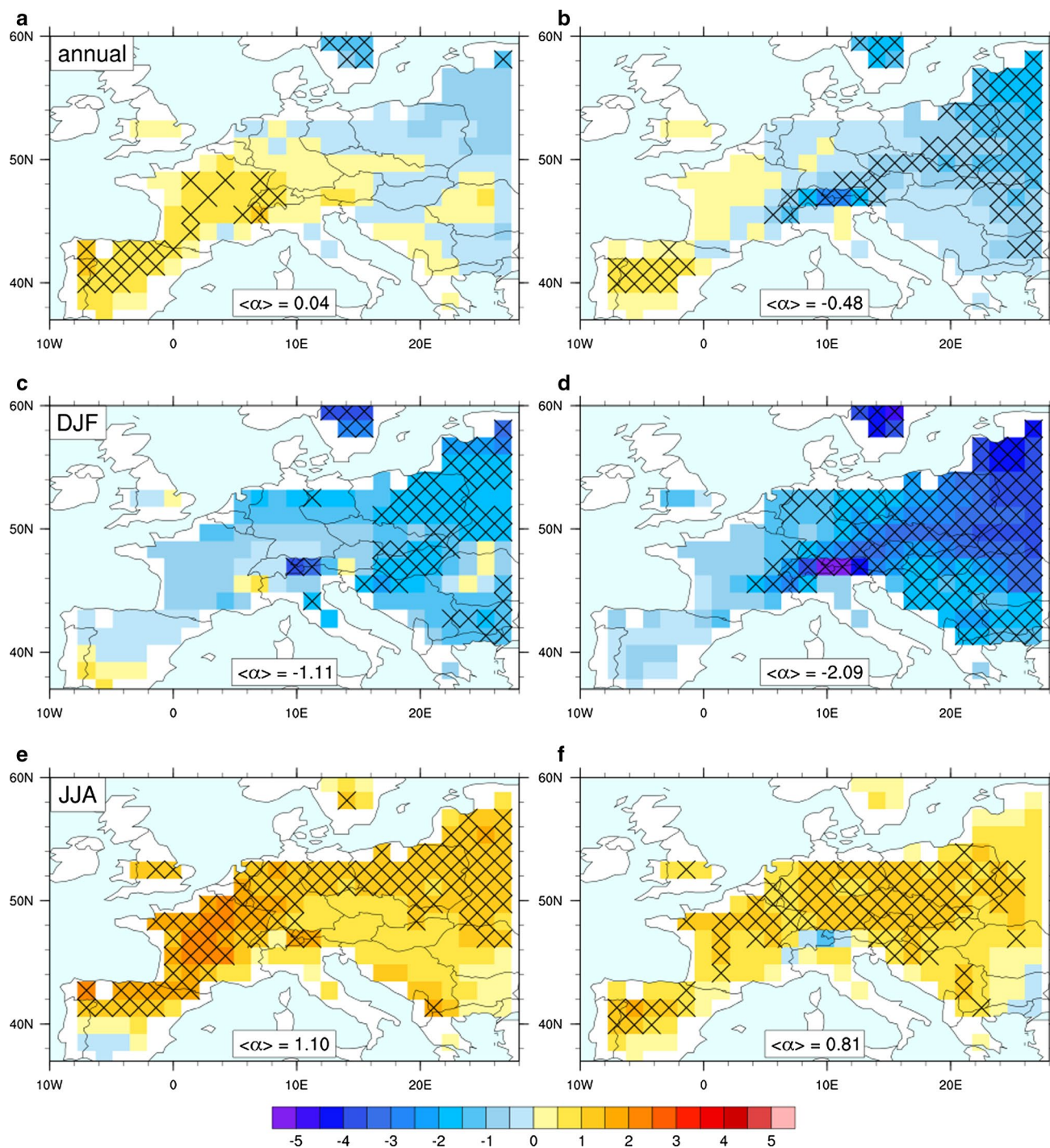


Fig. 10 Spatial distribution of the annual (a, b), winter (c, d) and summer (e, f) value of α from daily maximum (a, c, e) and minimum (b, d, f) surface temperatures. The α parameter has been calculated from 1956 to 2100 by combining the five historical simulations with

the subsequent RCP8.5 ones. Crosses indicate grid points where α is significantly different from 0 at the 10 % level. The average value of α over Europe is given in boxes

Over the twenty-first century, a strong increase in the sum of the number of summer upper records over southern Europe is projected to occur, with an acceleration of this rise from the 2050s onwards (Fig. 11a). This increase in

temperature extremes is partly due to a rise in mean daily maximum near-surface temperatures (Fig. 11b). Over the region, the mean temperature is projected to increase by 5 °C compared to the 1976–2005 climatology.

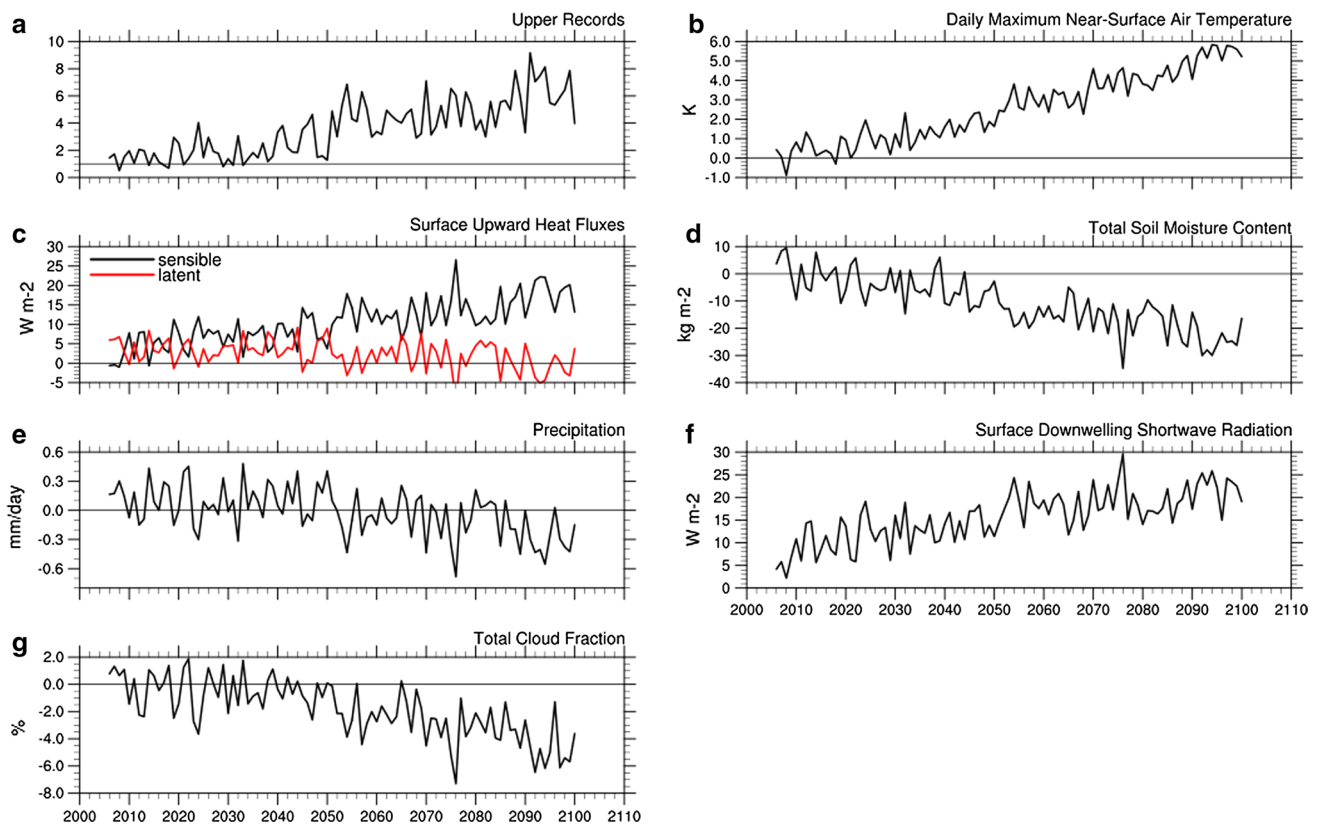


Fig. 11 Summer evolution over the twenty-first century of a set of variables in RCP8.5 ensemble mean, averaged over southern Europe (10°W – 28°E and 37 – 45°N). **a** Summer number of upper records summed over southern Europe, under the normalized form, where the expected record number in a stationary climate is 1. Anomalies are estimated relatively to the 1976–2005 period and using the ensemble

mean of the five related historical members for **b** daily maximum near-surface air temperature (K), **c** surface upward sensible (*black*) and latent (*red*) heat fluxes (W m^{-2}), **d** total soil moisture content (kg m^{-2}), **e** precipitation (mm day^{-1}), **f** surface downwelling shortwave radiation (W m^{-2}) and **g** total cloud fraction (%)

The second half of the twenty-first century is characterized by an important change in the evolution of surface heat fluxes (Fig. 11c). Indeed, from the 2050s onwards, the evolutions of the sensible and latent fluxes diverge, with a decrease in the latent flux and an increase in the sensible flux. This divergence suggests a change from a limitation of latent fluxes by the energy at the surface to a limitation by the soil moisture availability. Different processes could explain this change in regime. First, the total soil moisture content is projected to decrease during the twenty-first century, with a stronger decrease in the second half of the century (Fig. 11d). This progressive loss in soil moisture during summer can be linked to an antecedent decrease in soil moisture during the spring season and to a decrease of precipitation during summer (Fig. 11e). Second, the surface downwelling shortwave radiation is projected to increase over the twenty-first century, with a stronger increase in the second half of the century (Fig. 11f). This is mostly due to the decreasing total cloud fraction over the century (Fig. 11g), once again accentuated from the 2050s onward. The increase in shortwave radiation flux throughout the

period could also be linked to a decreasing concentration of aerosols since the 1990s, but to a lesser extent at the end of the century.

The divergence between the evolution of the sensible and latent heat fluxes can therefore be explained by the decrease in cloud cover and soil moisture. It is likely that changes in soil moisture and cloud cover are themselves related through a feedback loop. The decrease in atmospheric humidity and the increase in temperature potentially associated with a decrease in evapotranspiration induced by soil drying are expected to lead to a decrease in relative humidity. Condensation becomes more difficult to achieve, which is consistent with a decrease in cloud cover and also a decrease in precipitation, which in turn may impact soil moisture.

Consequently, from the 2050s onwards, the model projects that the surface will receive more solar energy, but also contain less moisture. The sensible heat flux is then projected to play a stronger role in the repartition of surface energy during the second half of the twenty-first century. In association with these changes, a strong increase in record-breaking warm temperatures is projected by the model.

6 Conclusion

Over the second half of the twentieth century, we cannot detect any statistically significant changes in the annual and seasonal evolutions of the upper and lower records over Europe. At the end of the twentieth century, the upper and lower record evolutions are still in the range of the model's internal variability. Yet, from the 1980s onwards, a change in the record evolution is observed and simulated. Daily minimum and maximum record-breaking temperatures tend to occur less and more often, respectively, than in a stationary climate.

Using single forcing simulations, we have shown that the response to the natural forcings alone is not representative of the observed and simulated (with all forcings applied) changes over the late twentieth century. Simulations forced by isolated anthropogenic forcings are capable of reproducing either the temporal or spatial distributions of these present-day numbers of records.

The projected record evolution over the twenty-first century under the RCP8.5 scenario exhibits a strong warming trend in the annual and seasonal evolutions of daily minimum and maximum record-breaking temperatures. At the end of the century, upper records are projected to occur on average five (to six, according to the season) times more often than during the 1960s and 1970s over Europe. In contrast, it is increasingly difficult to break a lower record. These changes are significantly inconsistent with the model's internal variability from the 2020s and 2030s onwards for the annual numbers of lower and upper records, respectively.

The spatial distribution of the increase in the annual number of upper records under the RCP8.5 shows a significant and homogeneous fivefold increase over Europe during the last three decades of the twenty-first century, compared to the expected record number in a stationary climate. This spatial distribution of upper records presents seasonally contrasted patterns. The Mediterranean region is particularly affected in summer, whereas central and northeastern Europe are more impacted in winter.

At the end of the current century, the spatial distribution of the averaged annual number of lower records presents values ten times lower than expected in a stationary climate, particularly over northern Europe. The spatial distribution of lower record occurrences once again illustrates the extreme difficulty involved in breaking new cold records whatever the day of the year at the end of the current century, but particularly in summer and winter.

In winter, the CNRM-CM5 model projects a negative trend in interannual variability over the 1956–2100 period for both minimum and maximum surface temperatures everywhere over Europe, but with significant results gathered over eastern Europe. In summer, an increase in interannual

variability is found homogeneously over Europe. Significant changes are found over northeastern Europe, France and northern Spain for daily maximum surface temperatures, whereas central Europe and central Spain present significant results for minimum temperatures.

Future work could extend this study to a set of independent CMIP5 models. Changes in the evolution of records could then be detected in a multimodel ensemble with regard to a larger sample to estimate the internal variability. The study of physical mechanisms in other models might help to better understand the processes responsible for extreme temperature changes over Europe. Regional models could also provide a more accurate representation of these extreme events due to an improved representation of land–sea and land–orographic effects.

Finally, a comparison between record-breaking temperatures and the evolution of extreme indices might provide additional information regarding the assessment of future extreme temperature events over Europe. Warm spell indices could, for example, indicate the evolution of the persistence of these extreme events, which is not included in record indices.

Acknowledgments This work is supported by EDF and by the French National Research Agency (ANR) and its program «Investissements d'avenir» under the Grant ANR-11-RSNR-0021. The authors thank Aurelien Ribes and Julien Cattiaux for their very helpful suggestions. All analyses and graphics have been done using the NCAR Command Language (NCL 2013).

References

- Anderson A, Kostinski A (2010) Reversible record breaking and variability: temperature distributions across the globe. *J Appl Meteorol Climatol* 49(8):1681–1691. doi:[10.1175/2010JAMC2407.1](https://doi.org/10.1175/2010JAMC2407.1)
- Barriopedro D, Fischer EM, Luterbacher J, Trigo RM, García-Herrera R (2011) The hot summer of 2010: redrawing the temperature record map of Europe. *Science* (New York, N.Y.) 332(6026):220–224. doi:[10.1126/science.1201224](https://doi.org/10.1126/science.1201224)
- Benestad RE (2003) How often can we expect a record event? *Clim Res* 25:3–13
- Benestad RE (2004) Record-values, nonstationary tests and extreme value distributions. *Glob Planet Change* 44(1–4):11–26. doi:[10.1016/j.gloplacha.2004.06.002](https://doi.org/10.1016/j.gloplacha.2004.06.002)
- Boé J, Terray L (2008) Uncertainties in summer evapotranspiration changes over Europe and implications for regional climate change. *Geophys Res Lett* 35(5):L05702. doi:[10.1029/2007GL032417](https://doi.org/10.1029/2007GL032417)
- Christiansen B (2013) Changes in temperature records and extremes: are they statistically significant? *J Clim* 26(20):7863–7875. doi:[10.1175/JCLI-D-12-00814.1](https://doi.org/10.1175/JCLI-D-12-00814.1)
- Coumou D, Rahmstorf S (2012) A decade of weather extremes. *Nat Clim Change*. doi:[10.1038/NCLIMATE1452](https://doi.org/10.1038/NCLIMATE1452)
- Coumou D, Robinson A, Rahmstorf S (2013) Global increase in record-breaking monthly-mean temperatures. *Clim Change* 118(3–4):771–782. doi:[10.1007/s10584-012-0668-1](https://doi.org/10.1007/s10584-012-0668-1)

- Della-Marta PM, Haylock MR, Luterbacher J, Wanner H (2007) Doubled length of western European summer heat waves since 1880. *J Geophys Res* 112(D15):D15103. doi:[10.1029/2007JD008510](https://doi.org/10.1029/2007JD008510)
- Elguindi N, Rauscher SA, Giorgi F (2012) Historical and future changes in maximum and minimum temperature records over Europe. *Clim Change* 117(1–2):415–431. doi:[10.1007/s10584-012-0528-z](https://doi.org/10.1007/s10584-012-0528-z)
- Fischer EM, Rajczak J, Schär C (2012) Changes in European summer temperature variability revisited. *Geophys Res Lett*. doi:[10.1029/2012GL052730](https://doi.org/10.1029/2012GL052730)
- Franke J, Wergen G, Krug J (2010) Records and sequences of records from random variables with a linear trend. *J Stat Mech*. doi:[10.1088/1742-5468/2010/10/P10013](https://doi.org/10.1088/1742-5468/2010/10/P10013)
- Gupta AS, Jourdain NC, Brown JN, Monselesan D (2013) Climate drift in the CMIP5 models*. *J Clim* 26(21):8597–8615. doi:[10.1175/JCLI-D-12-00521.1](https://doi.org/10.1175/JCLI-D-12-00521.1)
- Hansen J, Sato M, Ruedy R (2012) Perception of climate change. *Proc Natl Acad Sci USA* 109(37):E2415–E2423. doi:[10.1073/pnas.1205276109](https://doi.org/10.1073/pnas.1205276109)
- Haylock MR, Hofstra N, Klein Tank AMG, Klok EJ, Jones PD, New M (2008) A European daily high-resolution gridded data set of surface temperature and precipitation for 1950–2006. *J Geophys Res* 113(D20):D20119. doi:[10.1029/2008JD010201](https://doi.org/10.1029/2008JD010201)
- IPCC (2007) Climate change 2007: the physical science basis. In: Solomon S, Qin D, Manning M, Chen Z, Marquis M, Averyt KB, Tignor M, Miller HL (eds) Contribution of Working Group I to the fourth assessment report of the Intergovernmental Panel on Climate Change. Cambridge University Press, Cambridge, United Kingdom and New York, NY, 996 pp
- IPCC (2012) Managing the risks of extreme events and disasters to advance climate change adaptation. In: Field CB, Barros V, Stocker TF, Qin D, Dokken DJ, Ebi KL, Mastrandrea MD, Mach KJ, Plattner GK, Allen SK, Tignor M, Midgley PM (eds) A special report of Working Groups I and II of the Intergovernmental Panel on Climate Change. Cambridge University Press, Cambridge, UK, and New York, NY, 582 pp
- IPCC (2013) Climate change 2013: the physical science basis. In: Stocker TF, Qin D, Plattner G-K, Tignor M, Allen SK, Boschung J, Nauels A, Xia Y, Bex V, Midgley PM (eds) Contribution of Working Group I to the fifth assessment report of the Intergovernmental Panel on Climate Change. Cambridge University Press, Cambridge, United Kingdom and New York, NY, 1535 pp
- Katz RW, Brown BG (1992) Extreme events in a changing climate: variability is more important than averages. *Clim Change* 21:289–302
- Krug J (2007) Records in a changing world. *J Stat Mech Theory Exp* 2007(07):P07001–P07001. doi:[10.1088/1742-5468/2007/07/P07001](https://doi.org/10.1088/1742-5468/2007/07/P07001)
- Meehl GA, Tebaldi C, Walton G, Easterling D, McDaniel L (2009) Relative increase of record high maximum temperatures compared to record low minimum temperatures in the US. *Geophys Res Lett* 36(23):L23701. doi:[10.1029/2009GL040736](https://doi.org/10.1029/2009GL040736)
- NCL (2013) The NCAR command language (Version 6.1.2) [Software]. UCAR/NCAR/CISL/VETS, Boulder, Colorado. doi:[10.5065/D6WD3XH5](https://doi.org/10.5065/D6WD3XH5)
- Newman WI, Malamud BD, Turcotte DL (2010) Statistical properties of record-breaking temperatures. *Phys Rev E* 82(6):066111. doi:[10.1103/PhysRevE.82.066111](https://doi.org/10.1103/PhysRevE.82.066111)
- Parey S, Dacunha-Castelle D, Hoang TTH (2009) Mean and variance evolutions of the hot and cold temperatures in Europe. *Clim Dyn* 34(2–3):345–359. doi:[10.1007/s00382-009-0557-0](https://doi.org/10.1007/s00382-009-0557-0)
- Peters GP, Andrew RM, Boden T, Canadell JG, Ciais P, Le Quééré C, Marland G, Raupach MR, Wilson C (2012) The challenge to keep global warming below 2°C. *Nat Clim Change* 3(1):4–6. doi:[10.1038/nclimate1783](https://doi.org/10.1038/nclimate1783)
- Rahmstorf S, Coumou D (2011) Increase of extreme events in a warming world. *Proc Natl Acad Sci USA* 108(44):17905–17909. doi:[10.1073/pnas.1101766108](https://doi.org/10.1073/pnas.1101766108)
- Redner S, Petersen M (2006) Role of global warming on the statistics of record-breaking temperatures. *Phys Rev E* 74(6):061114. doi:[10.1103/PhysRevE.74.061114](https://doi.org/10.1103/PhysRevE.74.061114)
- Robine J-M, Cheung SLK, Le Roy S, Van Oyen H, Griffiths C, Michel J-P, Herrmann FR (2008) Death toll exceeded 70,000 in Europe during the summer of 2003. *CR Biol* 331(2):171–178. doi:[10.1016/j.crvi.2007.12.001](https://doi.org/10.1016/j.crvi.2007.12.001)
- Ruokolainen L, Räisänen J (2009) How soon will climate records of the 20th century be broken according to climate model simulations? *Tellus A* 61(4):476–490. doi:[10.1111/j.1600-0870.2009.00398.x](https://doi.org/10.1111/j.1600-0870.2009.00398.x)
- Schär C, Vidale PL, Lüthi D, Frei C, Häberli C, Liniger MA, Appenzeller C (2004) The role of increasing temperature variability in European summer heatwaves. *Nature* 427(January):3926–3928. doi:[10.1038/nature02230.1](https://doi.org/10.1038/nature02230.1)
- Scherrer SC, Apenzeller C, Liniger MA, Schär C (2005) European temperature distribution changes in observations and climate change scenarios. *Geophys Res Lett* 32(19):L19705. doi:[10.1029/2005GL024108](https://doi.org/10.1029/2005GL024108)
- Seneviratne SI, Lüthi D, Litschi M, Schär C (2006) Land–atmosphere coupling and climate change in Europe. *Nature* 443(7108):205–209. doi:[10.1038/nature05095](https://doi.org/10.1038/nature05095)
- Shindell DT, Schmidt GA (2004) Dynamic winter climate response to large tropical volcanic eruptions since 1600. *J Geophys Res* 109(D5):D05104. doi:[10.1029/2003JD004151](https://doi.org/10.1029/2003JD004151)
- Terray L, Boé J (2013) Quantifying 21st-century France climate change and related uncertainties. *CR Geosci* 345(3):136–149. doi:[10.1016/j.crte.2013.02.003](https://doi.org/10.1016/j.crte.2013.02.003)
- Trewin B, Vermont H (2010) Changes in the frequency of record temperatures in Australia, 1957–2009. *Aust Meteorol Oceanogr J* 60:113–119
- Van Vuuren DP, Eickhout B, Lucas PL, den Elzen MGJ (2006) Long-term multi-gas scenarios to stabilise radiative forcing: exploring costs and benefits within an integrated assessment framework. *Energy J* SI2006(01):201234. doi:[10.5547/ISSN0195-6574-EJ-VolSI2006-NoSI3-10](https://doi.org/10.5547/ISSN0195-6574-EJ-VolSI2006-NoSI3-10)
- Van Vuuren DP, Elzen MGJ, Lucas PL, Eickhout B, Strengers BJ, Ruijven B, Houdt R (2007) Stabilizing greenhouse gas concentrations at low levels: an assessment of reduction strategies and costs. *Clim Change* 81(2):119159. doi:[10.1007/s10584-006-9172-9](https://doi.org/10.1007/s10584-006-9172-9)
- Voltaire A, Sanchez-Gomez E, Salas y Méria D, Decharme B, Casou C, Sénési S, Valcke S, Chauvin F (2012) The global climate model: description and basic evaluation. *Clim Dyn* 40(9–10):2091–2121. doi:[10.1007/s00382-011-1259-y](https://doi.org/10.1007/s00382-011-1259-y)
- Wergen G, Krug J (2010) Record-breaking temperatures reveal a warming climate. *EPL (Europhys Lett)* 92(3):30008. doi:[10.1209/0295-5075/92/30008](https://doi.org/10.1209/0295-5075/92/30008)
- Wergen G, Hense A, Krug J (2014) Record occurrence and record values in daily and monthly. *Clim Dyn* 42(5–6):1275–1289
- Wigley TML (2000) ENSO, volcanoes and record-breaking temperatures. *Geophys Res Lett* 27(24):4101–4104. doi:[10.1029/2000GL012159](https://doi.org/10.1029/2000GL012159)
- Wild M (2011) Enlightening global dimming and brightening. *Bull Am Meteorol Soc* 93(1):27–37. doi:[10.1175/BAMS-D-11-00074.1](https://doi.org/10.1175/BAMS-D-11-00074.1)